



OPEN

Biosynthesis of copper oxide nanoparticles mediated *Annona muricata* as cytotoxic and apoptosis inducer factor in breast cancer cell lines

Rana I. Mahmood¹, Afraa Ali Kadhim², Sumayah Ibraheem³, Salim Albukhaty^{4,5✉}, Harraa S. Mohammed-Salih⁶, Ruaa H. Abbas⁷, Majid S. Jabir⁸, Mustafa K. A. Mohammed⁹, Uday M. Nayeef⁸, Faizah A. AlMalki¹⁰, Ghassan M. Sulaiman⁸ & Hassan Al-Karagoly¹¹

This study investigated for the first time a simple bio-synthesis approach for the synthesis of copper oxide nanoparticles (CuO NPs) using *Annona muricata L.* (*A. muricata*) plant extract to test their anti-cancer effects. The presence of CuONPs was confirmed by UV-visible spectroscopy, Scanning electron microscope (SEM), and Transmission electron microscope (TEM). The antiproliferative properties of the synthesized nanoparticles were evaluated against (AMJ-13), (MCF-7) breast cancer cell lines, and the human breast epithelial cell line (HBL-100) as healthy cells. This study indicates that CuONPs reduced cell proliferation for AMJ-13 and MCF-7. HBL-100 cells were not significantly inhibited for several concentration levels or test periods. The outcomes suggest that the prepared copper oxide nanoparticles acted against the growth of specific cell lines observed in breast cancer. It was observed that cancer cells had minor colony creation after 24 h sustained CuONPs exposure using (IC_{50}) concentration for AMJ-13 was ($17.04 \mu\text{g mL}^{-1}$). While for MCF-7 cells was ($18.92 \mu\text{g mL}^{-1}$). It indicates the uptake of CuONPs by cancer cells, triggering apoptosis. Moreover, treatment with CuONPs enhanced Lactate dehydrogenase (LDH) production, probably caused by cell membrane damage, creating leaks comprising cellular substances like lactate dehydrogenase. Hence, research results suggested that the synthesized CuONPs precipitated anti-proliferative effects by triggering cell death through apoptosis.

In the past several years, the domain of material science has extensively focused on synthesizing nanoparticles with changeable morphology and defined dimensions, shape, and order. Much research has been conducted concerning nanoparticles and their immense applications for biosensing and chemo, energy conserving devices, drug delivery mechanisms, catalysis and electrochemistry, optoelectronics, optics, and medicinal therapeutics antibacterial, anticancer, and antimicrobial agents¹⁻⁴. Nanoscale size, distinct shape, and extensive surface area are advantages for their marked catalytic characteristics. Using post-functionalization techniques, additional surface changes for the materials create distinctive physical characteristics⁵. Numerous physical and chemical methods are being assessed for synthesizing NPs using bottom-up or top-down approaches⁶. However, a majority

¹Department of Biomedical Engineering, College of Engineering, Al-Nahrain University, Baghdad, Iraq. ²Department of Biology, College of Science, Mustansiriyah University, Baghdad, Iraq. ³Al_kindy College of Medicine, University of Baghdad, Baghdad, Iraq. ⁴Department of Chemistry, College of Science, University of Misan, Maysan 62001, Iraq. ⁵College of Medicine, University of Warith Al-Anbiyyaa, Karbala, Iraq. ⁶Department of Orthodontics, College of Dentistry, University of Baghdad, Baghdad 10011, Iraq. ⁷College of Dentistry, Al-Farahidi University, Baghdad, Iraq. ⁸Department of Applied Sciences, University of Technology, Baghdad 10066, Iraq. ⁹Department of Medical Physics, Al-Mustaqbal University College, Babylon 51001, Iraq. ¹⁰Department of Biology, College of Science, Taif University, P.O. Box 11099, Taif 21944, Saudi Arabia. ¹¹Department of Internal and Preventive Medicine, College of Veterinary Medicine, University of Al-Qadisiyah, Al Diwaniyah 58002, Iraq. ✉email: albukhaty.salim@uomisan.edu.iq; 100131@uotechnology.edu.iq

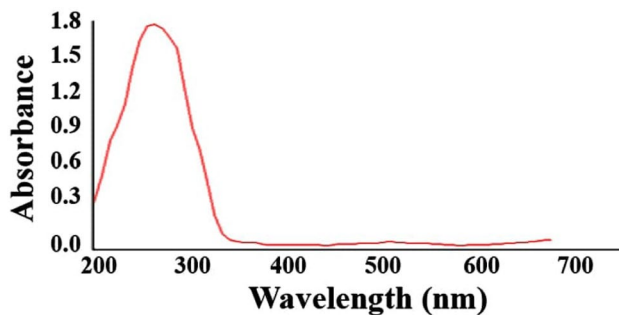


Figure 1. UV-spectroscopy of CuONPs.

of synthetic techniques require severe conditions with high temperature and pressure and potent reducing substances, producing nefarious by-products *in-situ*, which are discouraged by green protocols^{7,8}. Several scenarios use cost-intensive and challenging techniques. Hence, the demand for eco-friendly nanotechnology is increasing to facilitate the benefits of clean, biometric, and ecological processes for nanoparticle production^{9,10}.

Biological techniques for synthesizing NPs using plant leaf extracts or organisms like fungi, bacteria, and algae are considered eco-friendly substitutes for chemical synthesis because such approaches are nontoxic and less cost- and energy-intensive¹¹. Plant extract-based NP production approaches are more beneficial than environmentally friendly biological approaches because cell cultures are not required¹². Moreover, NP production using plants is beneficial because of safe handling and easy availability associated with plants and their extensive metabolite content to facilitating reduction¹³.

MCF-7 is an adherent, epithelial cell regarded One of the most important contributions of the MCF-7 cell line to breast cancer research has been its utility for the study of the estrogen receptor (ER) alpha, as this cell line is one of a very few to express substantial levels of ER mimicking the majority of invasive human breast cancers that express ER¹⁴. Plants contain many phytochemicals and synthesize several secondary metabolites that are potentially usable for Cu and CuO NPs production. Flavonoids and phenols are among the vital phytochemicals present in different plant parts like roots, leaves, flowers, shoots, stems, and fruits. Such phenolic substances contain ketone and hydroxyl groups, facilitating iron chelation and possessing potent antioxidant characteristics^{15,16}. NPs produced using this green approach enhance stability, reduce deformation and aggregation of NPs, and facilitate phytochemical adsorption from NP surface, contributing to higher reaction speed¹⁷. Research works suggest that plant-based Cu/CuO NPs exhibit antitumor properties for colon¹⁸, breast¹⁸, blood (leukemia)¹⁸, liver¹⁹, cervical²⁰, ovarian, skin (epithelioma)²¹, lung²¹, and gastric cancers²². *Annona muricata L.* (*A. muricata*) from the Annonaceae family has been extensively researched in the last few decades because of its therapeutic benefits. The use of Annonaceae family plants for medicinal benefits has been suggested long back; consequently, these species have been researched extensively because of their traditional uses and potent bioactivity^{23,24}. Medicinal plants are regarded as essential for healthcare benefits globally. Chronic degenerative conditions have assumed epidemic proportions; these are severe health concerns, causing treatment options to be given due clinical attention²⁵. Data about specific cytotoxic characteristics of *A. muricata* reported ethnobotanically has raised the species' popularity as an antitumor agent²⁶. In-vitro studies indicated that extracts affected cancerous cells more immensely than normal cells; most extracts did not cause cytotoxicity for healthy human cells, indicating selectivity²⁷. Experiments indicated that *A. muricata* leaf-based hydroalcoholic extracts with 1.6 mg/mL and 50 mg/mL concentrations enhanced non-tumor cell viability, while 100 mg/mL did not change viability²⁸. Reports suggest such selectivity speeds healing without many side effects. The present study was conducted by employing *A. muricata* as a reducing agent to synthesize CuO nanoparticles and assess potential therapeutic anticancer activity.

Results and discussion

Characterizing the synthesised CuONPs. Exposure to *A. muricata* peel extract was used to prepare CuO NPs, assessed using UV spectroscopy. As depicted in Fig. 1, the prepared CuONPs peaked around 260 nm^{29,30}.

SEM imaging outcomes indicated that prepared nanoparticles' diameter ranged between 33.24 ± 6.49 nm (Fig. 2A,B). Dispersed spherical nanoparticles were evaluated for Brownian movement using DLS assay, which helped understand the correlation between NPs' hydrodynamic length characteristics inside the dispersing medium. Mathematical calculations of light scattering intensity dynamics are vital to understanding the correlation between NPs' hydrodynamic length. As depicted in Fig. 2C, the prepared CuONPs had a 16–31 nm diameter range.

CuONPs increase in lactate dehydrogenase release. The lactate dehydrogenase enzyme regulates the lactate-pyruvate transformation, which is critical for cellular energy production. Cell membrane integrity reduces when specific treated cells are introduced to this enzyme in the culture medium. LDH evaluation was used to determine the cytotoxic aspects of CuONPs on processed cells. Cell damage is followed by the cytoplasmic release of lactate dehydrogenase, triggering the conversion of the tetrazolium salt into formazan. Formazan formation is assessed using 490 nm, indicating the fraction and count of injured, affected, or dying cells. The gathered information could indicate CuONPs' ability to enter the treated cells, trigger vesicle development, and

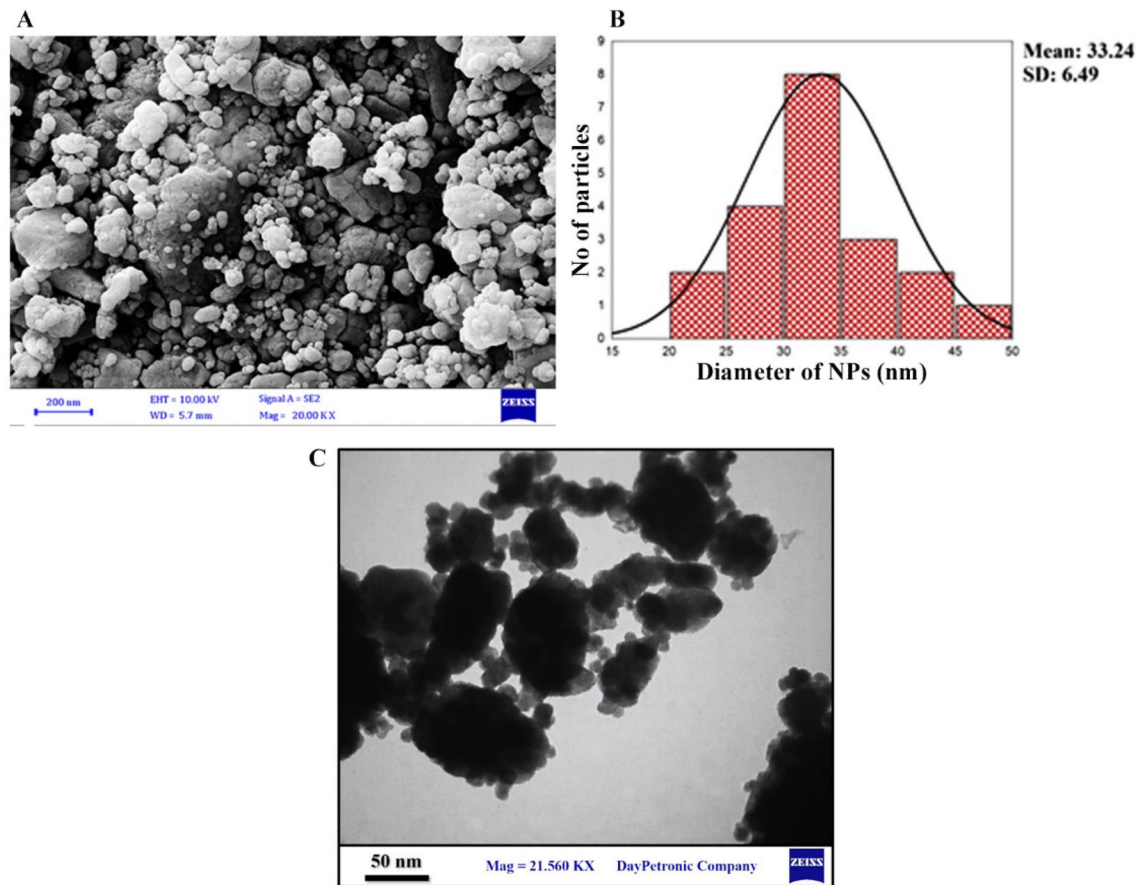


Figure 2. Structural and Morphological Properties of CuO NPs. (A) SEM image. (B) Diameter (nm) of CuONPs ranged between 33.24 ± 6.49 nm. (C) TEM image.

enter them. Figure 3 indicates CuONPs' capability to enhance LDH release, which is time-specific. CuO nanoparticles can penetrate cells and other biological components, leading to significant cellular degradation and triggering LDH production. At the same time, cells might consume 100–200 nm nanoparticles, triggering toxic phenomena like genetic changes and DNA damage.

Nanoparticle toxicity might be associated with processes that increase oxidative stress by interfering with the antioxidant system³¹. Free radicals such as ROS damage several membranes like those protecting the cell and mitochondria. Consequently, cellular constituents such as proteins, fatty acids, lipids, and nucleic acids, cause cellular death, reducing the proper functioning of the electronic transport mechanism. AMJ-13 and MCF-7 cells' cytotoxicity might be associated with oxidative-stress caused cellular degradation. Moreover, time-based LDH production triggered by CuONPs exposure might be associated with the cell membrane. Along the same lines, time-based LDH production increase triggered by CuONPs might be associated with cellular membrane destruction, leading to the leakage of cellular enzymes like lactate dehydrogenase. Cytotoxicity initiation observed in this study aligns with the conclusions³².

Anti-proliferative activity of CuONPs. We evaluated the cytotoxic aspects of the synthesized CuONPs on HBL-100, AMJ-13, and MCF-7. The CuONPs' antitumor characteristics were assessed by evaluating the degree of proliferation inhibition concerning malignant cells. The outcomes indicated extremely toxic significant effects exerted by the synthesized CuONPs on AMJ-13 and MCF-7 cells.

While the outcomes did not indicate CuONPs induced cytotoxicity for the healthy cells (HBL-100), anticancer phenomena were detected by evaluating nanoparticles' capability to reduce or block cancer cells, as depicted in Fig. 4. Hence, CuONPs can reduce cancer cell growth. AMJ-13 and MCF-7 lines were similarly impacted due to CuONPs exposure. The outcomes indicate the capability of CuONPs to reduce the proliferation of cancer cell lines. A 72-h CuONPs treatment provided to cancer cells significantly reduced proliferation capability, which aligns well with previous study outcomes³³. In a study by Naik and Sellappan³⁴, it was discovered that two *A. muricata* extracts showed higher genotoxic potential on breast cancer (MCF-7) cells when assessed using the alkaline comet assay. In another study, the ability of methanol extracts of *Annona muricata* leaves to induce apoptosis and/or stop the cell cycle was investigated in an effort to discover a potential strategy for controlling or inhibiting the growth of MCF-7 breast cancer³⁵. CuO NPs demonstrated a wide range of cytotoxicity in our MTT cytotoxicity screening assay, with the majority of activity on AMJ-13 and MCF-7 cells but not on normal HBL-100 cells. The difficulty of anticancer medications to accurately differentiate cancer cells is one of the major problems facing cancer chemotherapy. Although CuO's cancer-specific toxicity is still unclear, CuO NPs' ability to

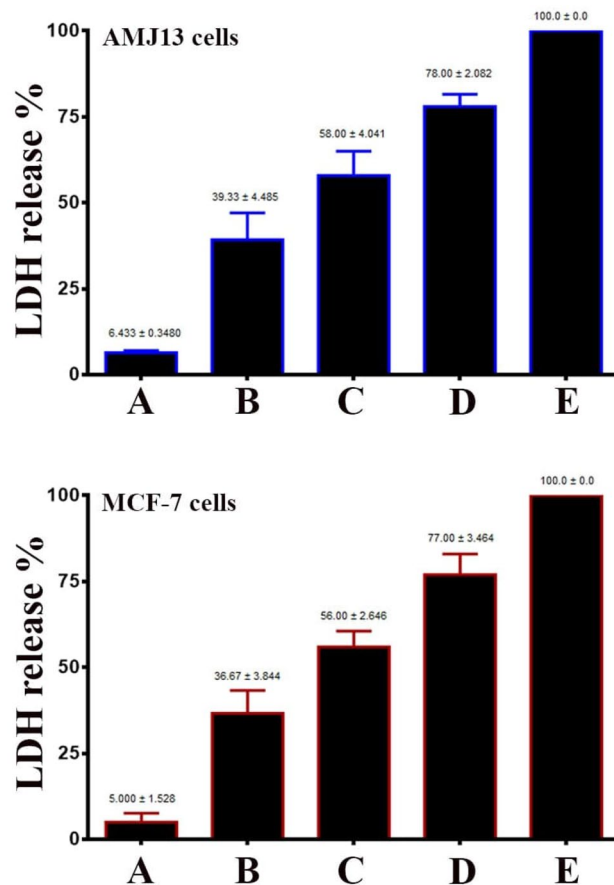


Figure 3. CuO NPs increase the release of lactate dehydrogenase (LDH) production. (A) control untreated cells. (B) Cells treated with 25 $\mu\text{g mL}^{-1}$ of CuO NPs. (C) Cells treated with 50 $\mu\text{g mL}^{-1}$ of CuO NPs. (D) Cells treated with 100 $\mu\text{g mL}^{-1}$ of CuO NPs. 1% Triton-x was employed for positive control reference (E). LDH release was measured at 490 nm. Results are represented as mean \pm SD.

selectively destroy cancer cells has clinical significance³⁶. Recently, selective cytotoxicity of other nano-particles including gold nanoparticles (Au NPs) and silver nanoparticles (Ag NPs) on cancerous cells has been reported. Khorrami et al. observed that Ag NPs nanoparticles with an average size of 31.4 nm exhibited a preferential ability to kill MCF-7 cancerous cells as compared to normal L-929 fibroblast cells³⁷. Vetten et al. indicated that AuNPs with an average size of 20 nm were considerably more toxic to Chinese hamster ovary cells in comparison to the same nanoparticles with the size of 14 nm³⁸. Current findings in cancer research imply that the production of reactive oxygen species (ROS) through oxidative stress is a major method shared by multiple apoptotic stimuli¹⁹. ROS has been identified as an important signaling molecule for the start and completion of apoptosis¹⁹. Oxidative stress has shown the toxicity of CuO NPs in many human cell lines, including human lung epithelial (A549), human heart microvascular endothelial (HCMEC)³⁹, and human hepatocarcinoma cell line (HepG2)⁴⁰. CuO NPs' cytotoxicity towards mammalian cells varies depending on the kind of cell.

Tumor cell colony development reduced after sustained CuONPs exposure for 24 h using (IC_{50}) concentration, indicating that the cells were destroyed (Fig. 5). Hence, there was nanoparticle uptake at the cellular level, triggering apoptosis. Hence, the outcomes indicate that CuONPs are capable of triggering cell death. These results demonstrate that CuONPs selectivity reduces AMJ-13 and MCF-7 cell proliferation. The biomolecules in the plant extract function as efficient capping agents, hence facilitating the synthesis of NPs. NPs appear to be stabilized by a diverse range of mechanisms, notably electrostatic stability, steric stability, hydration force stability, and van der Waals forces. The stability of nanoparticles is crucial for their functions and applications⁴¹. Different processes, including apoptosis and necrosis⁴², can be utilized by NPs to inhibit cell viability. The induction of tumor cell apoptosis is an essential mechanism for anti-cancer agents^{43,44}. The process of apoptosis, marked by morphological and biochemical changes, and the apoptosis of distinct cells in the same tissue do not occur simultaneously. Copper oxide nanoparticles demonstrated a concentration-dependent cytotoxic impact against breast cancer cells in our investigation.

CuoNPs triggered apoptosis in breast cancer cells. Apoptosis is a vital homeostasis phenomenon that regulates different cell category concentrations⁴⁵. The working hypothesis is that the synthesized CuONPs trigger apoptosis for processed AMJ-13, and MCF-7, indicating anti-proliferative characteristics. We evaluated if

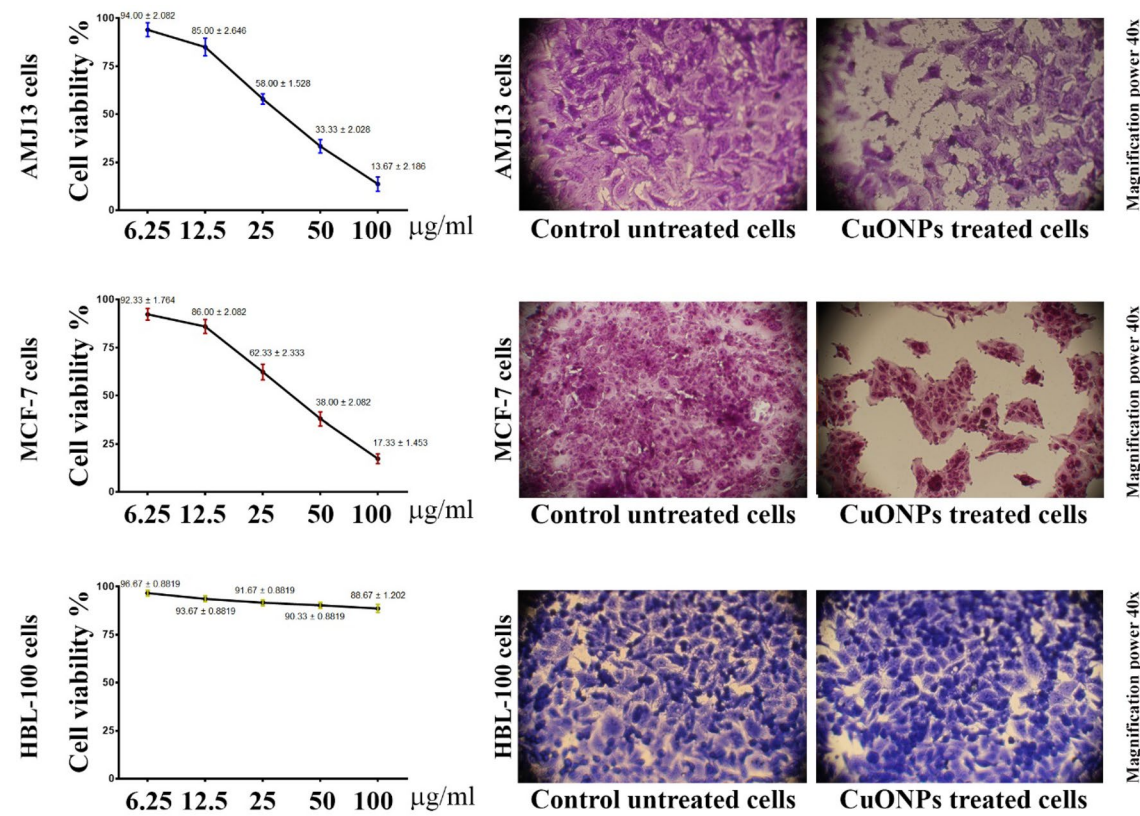


Figure 4. The Antiproliferative activity of CuO NPs against cancer cell lines. Triplicate samples of AMJ-13, MCF-7, and HBL-100 cells at a concentration of 1×10^4 cells mL^{-1} were seeded. CuO NPs were added to these samples and incubation periods for 72 h. Cells were stained with MTT. The 492 nm wavelength was selected to assess absorbance.

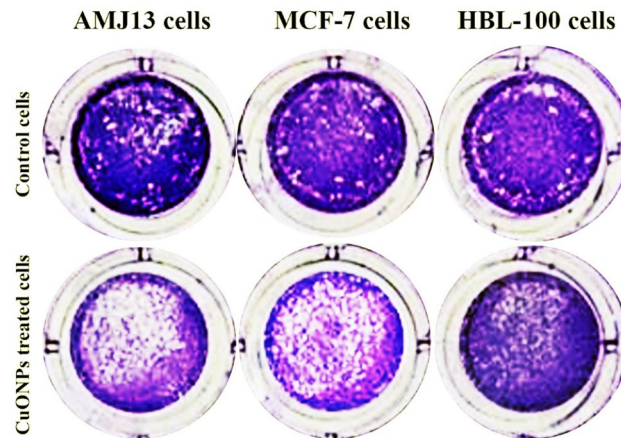


Figure 5. CuONPs inhibit the Colony-forming of MCF-7 and AMJ-13. A 24-h CuONPs treatment was provided at IC₅₀ concentration, followed by crystal violet staining for 20 min.

the nanoparticles triggered anti-proliferative activity concerning AMJ-13 and MCF-7 breast cancer cell lines and normal (HBL-100) lines for human cells concerning apoptosis triggers. The cells were treated using CuONPs at (IC₅₀) concentration. The Ao/EtBr dual stain comprises fluorescent compounds mixed for identifying morphological transformation concerning the nucleus, providing distinct fluorescence.

The AMJ-13 and MCF-7 cells were exposed to CuONPs at IC₅₀ levels for 24 h, followed by dual staining and visual assessment using fluorescence microscopy to ascertain nuclear structure change, as depicted in Fig. 6A. Therefore, tumor cells were exposed to CuONPs, indicating damage to the cell membrane and lysosome vacuoles compared to unexposed lines. No changes were identified for healthy cells. The outcomes demonstrated that CuONPs possessed potent cell-death triggering potential, which might be due to the significant membrane

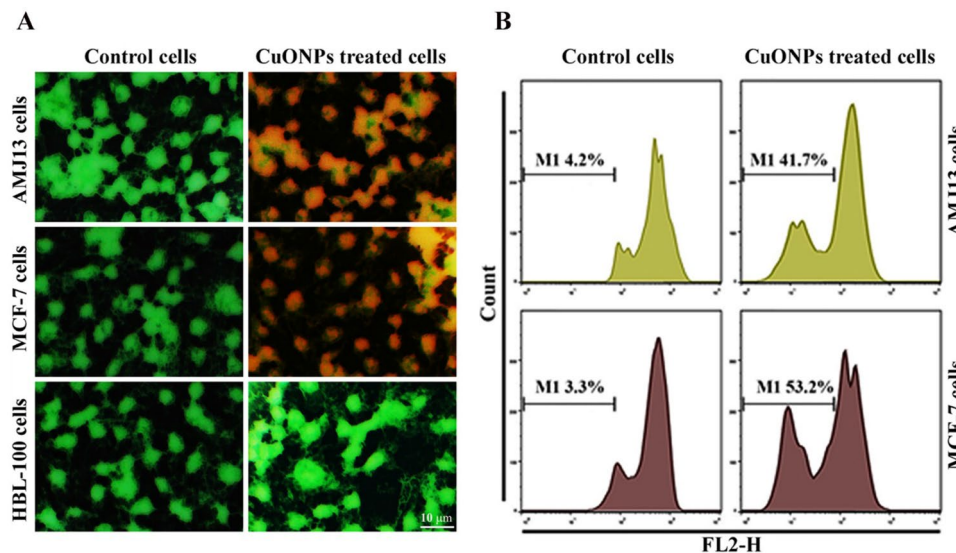


Figure 6. Apoptosis markers in cancer cells after treatment with CuO NPs. **(A)** Apoptotic indicators for AMJ-13, MCF-7, and HBL-100 cells exposed to CuONPs at IC_{50} concentrations for 24 h and stained for 2 min using AO/EtBr. Unexposed cells have an intact structure. Nevertheless, CuONPs exposure correlated with apoptotic aspects indicated using red stains. Scale bar 10 μ m. **(B)** Cells cycle phase. Sub-G₁ phase concerning MCF-7 and AMJ-13 cells' flow cytometry.

breaching ability. Ethidium bromide and acridine orange dyes were mixed to comprehensively assess the degree to which CuONPs could trigger the death of tumor cells. The outcomes reflected a bright green tinge, suggesting an undamaged nucleus. Nanoparticle-treated tumor cells had reduced cell membrane integrity compared to the control samples. Orange and red colors are characteristic of apoptotic cells. The present study also comprised experiments to assess the probable apoptosis-inducing ability of CuO NPs.

The constituent DNA was evaluated concerning the sub-G₁ phase through flow cytometry; subsequently, PI was used to stain the DNA of processed AMJ-13 and MCF-7 cells. The sub-G₁ phase outcomes suggested that the fraction of CuONPs-processed tumor cells rose to 41.7% from 4.2%, while MCF-7 cells increased to 53.2% from 3.3% (Fig. 6B). Study outcomes indicated that CuONPs demonstrated anti-proliferation characteristics by triggering cell death through apoptosis.

CuONPs triggered upregulation of caspase-3 and caspase-9 expressions. The previously-tested assay suggests that CuONPs can trigger mitochondria-specific apoptosis, which requires two primary techniques: intrinsic (mitochondria-level regulation) and extrinsic (death receptor-mediated). The extrinsic pathway comprises molecule surface signals (Fas/FasL), causing the inclusion of the Fas-associated death domain (FADD)⁴⁶. Caspases work in alignment with apoptosis triggers. The two major apoptosis pathways comprise the caspase-9 mediated mitochondrial and caspase-8 triggered death receptor pathways. Subsequently, executioner caspases -3 and -7 are triggered. The observations indicated significantly higher Caspase-3 and Caspase-9 levels (Fig. 7).

Materials and methods

Preparation of extracts. All the plant experiments were in compliance with relevant institutional, national, and international guidelines and legislation. The extraction protocol was performed according to Hemalatha et al.⁴⁷ After the fruits were collected, the outer epicarp was peeled off, their seedless endocarp was shade dried, and 50 g of the dried endocarp was macerated into a powder. The fruit powder was combined with hot, boiling, distilled water, and kept in a shaker at 200 rpm for 4 h at 37 °C to create a 5% (w/v) suspension. The suspension was next cooled to room temperature before being passed through four layers of No. 1 Whatman filter paper and a 0.22 m filter (Millipore, Sigma). After being filtered, the aqueous extract was freeze-dried, and the powder was kept at – 20 °C until use.

Cells and reagents. AMJ-13 (Iraqi patient's breast cancer cell line), MCF7, is an epithelial cell line isolated from the breast tissue of a patient with metastatic adenocarcinoma, and The HBL-100 cell line is an epithelial cell line derived in vitro from the milk of an apparently healthy woman. All cell lines were provided by the Iraqi Centre for Cancer and Medical Genetic Research (ICCMGR), Al-Mustansiriyah University, Baghdad, Iraq, which supplied the cells for the experiment. Trypsin-EDTA, fetal bovine serum, dimethyl sulfoxide (DMSO), RPMI-1640, 3-(4,5-Dimethylthiazol-2-yl)-2,5-diphenyltetrazolium bromide (MTT), and Triton X-100 were obtained from MO, USA. Kirkegaard & Perry Laboratories, Inc. (KPL) (Gaithersburg, MD, USA), while the other substances and reagents were analytical grade.

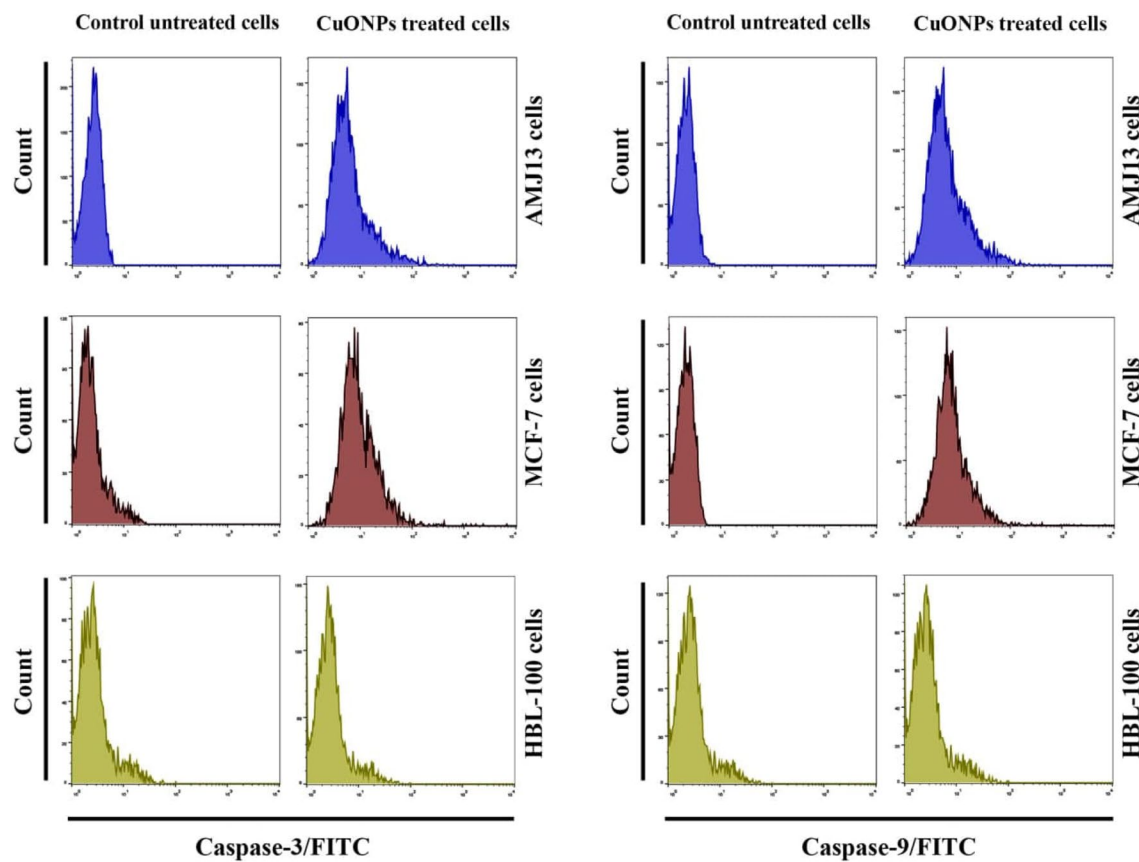


Figure 7. CuONPs up-regulated Caspase-3 and Caspase-9 expression. Flow cytometry was used to analyse fluorescence histograms of immunolabeled caspase-3 and caspase-9.

Culturing of cell lines. All cell lines were cultured in PRMI-1640 (Sigma, USA) media, which contained 10% fetal bovine serum (FBS), 100 units/mL of penicillin, and 100 g/mL of streptomycin (Capricorn Scientific GmbH, Ebsdorfergrund, Germany). The cell lines were first cultivated as adherent monolayers grown at 37 °C in an incubator with 5% CO₂ and a humidity atmosphere trypsinization for a short time using trypsin-EDTA (Capricorn Scientific GmbH, Ebsdorfergrund, Germany). These cells are routinely tested and verified.

Collection and phytochemical extraction of *A. muricata*. In this study, the plant *Annona muricata* used in this study is not a globally threatened species. It was prepared by the department of biotechnology/university of Technology from the local market in the city of Baghdad/Iraq. The phytochemical extraction was performed using 2 L chilled disinfected deionized distilled water mixed with 500 g *A. muricata* peel. To facilitate phytochemical removal uniformity, the sample was subjected to periodic vortexing during the 120-h standing period. Whatman filters (size 1) were used for staining the aqueous solution using a vacuum pump. A 4000-efficient Heldolph Laborata rotary evaporation apparatus was used for vacuum-based concentration for 12 h at 40 °C. Evaporation apparatus was used to dry the concentrates, and a powder form was obtained by treating the samples in hot air ovens set at 40 °C. The dry powder specimens obtained from the peel extracts were preserved at 4 °C using dark containers until used.

Green synthesis of copper oxide nanoparticles mediated *A. muricata* peel. A conical flask was filled with 98 ml aqueous solution of 120.8 mg Copper II Nitrate mixed with 1000 mL deionised distilled water (0.5 mM). 2 ml *Annona muricata* extract was added for copper nanoparticle biosynthesis. Aluminium foil was used to seal the conical flasks stored in dark chambers at room temperature (25–26 °C) for 24 h. Subsequently, all liquids were removed at 120 °C using a hot air oven. The burnt brown content was removed from the beakers; a spatula was used to fill Eppendorf tubes with 1.5 ml solution, stored between 25 and 30 °C.

Copper nanoparticle characterisation. *UV-Vis spectroscopy.* A Jenway 6715 UV-Vis spectrophotometer was employed for spectrophotometric assessment. Setups one and two were used to obtain 1 ml specimens after 8 and 24 h, respectively, and stored in separate cuvettes. The spectrophotometer was set at 1 nm resolution for the 200–700 nm range for assessing the prepared samples in order to determine the optical characteristics of copper nanoparticles.

Scanning electron microscopy SEM and TEM. The Carl Zeiss Sigma equipment was used for field emission scanning electron microscopy (FESEM) at 5.0 kV to determine the microstructure, and particle size characteristics of the CuONPs produced using the green approach. A carbon ribbon was taken, and 1 mg of copper nanoparticles were laid as a thin film coated using carbon, and several magnifications were used to capture the images. ImageJ software was employed to assess nanoparticle size distribution based on FESEM images.

Lactate dehydrogenase release assay. Manufacturer recommendations were followed to test the lactate dehydrogenase (LDH) producing activity specimen. CuONPs were used to treat the cells for 24-, 48- and 72-h periods. The processed cells' supernatant was moved onto a 96-well plate to assess LDH release characteristics by determining optical density at 490 nm⁴⁸.

MTT assay. A previously study was used to conduct the cytotoxicity test⁴⁹. RPMI-provided microtiter plates were used for cell seeding using 1×10^5 cells mL⁻¹ concentration. The plates were adhered overnight; subsequently, several CuONPs concentrations were used. The triplicate samples were incubated for 72-h periods. MTT solution was then used to treat cells incubated for a predetermined period. Medium aspiration and DMSO addition were performed to assess absorbance (492 nm) using a microplate instrument. Regression assessment was employed to determine the concentration-specific to 50% cell growth inhibition (IC_{50})^{50,51}.

Clonogenicity assay. The experiment comprised 24-well plates to create AMJ-13, HBL-100, and MCF-7 cell cultures (10^5 cells mL⁻¹ for 24 h and subsequent CuONPs treatment). Once monolayer confluence was achieved, the cells were isolated from the medium, followed by PBS rinsing. Crystal violet (Sigma-Aldrich, MO, USA) was used to stain fixed cells, then dye removal by washing, and photography⁵².

Acridine orange–ethidium bromide staining. Cells treated with copper nanoparticles were assessed for apoptosis induction using AO/EtBr staining (Sigma-Aldrich, USA). 12-well plates were used for cell seeding for 24 h; subsequently, copper nanoparticle treatment was used. PBS was used for two cell washing cycles. Solutions were prepared comprising identical cell volume and dual fluorescent dyes (10 μ L) to assess the specimens using fluorescence microscopy^{52,53}.

Flow cytometry assay for apoptotic cells. A cell cycle phase identification kit was used to identify sub-G1 cells. HBL-100, AMJ-13, and MCF-7 cell plating were conducted at 1×10^6 cell mL⁻¹ concentration. CuONPs treatment was provided to the cells for 24 h, followed by centrifugation, PBS washing, fixing, and resuspension using propidium iodide (PI) and RNase A based staining buffer. The sub-G1 peak was identified using the flow cytometer's FL2 channel⁵³.

Caspase-3 and caspase-9 level determination. Caspase-3 and caspase-9 activation states were assessed using fluorescent staining kits (Thermo Fisher Scientific, USA). The experiment comprised a 5 ml medium used to culture 4×10^4 cells mL⁻¹ SKOV-3 cancer cells, incubated at 37 °C for 24 h. Subsequently, the incubated specimens were treated with every compound for 24 h using 10 μ g mL⁻¹ concentration. Post-incubation, cells were removed, and 1 \times ice-cold PBS was used to wash the samples twice. The pellets were gathered, and the growth medium was used to change cell density to 1×10^6 cells mL⁻¹. Subsequently, 1 mL of FITC-IETD-FMK was used to treat the cultivated cells, which were incubated for 60 min at 37 °C, to pinpoint caspase-9 and caspase-3. After incubation, a wash buffer (0.5 mL) was used twice to clean the cell samples. The stained samples were placed inside flow cytometry tubes to start the cytometry process. BD Accuri C6 software was used to assess the gathered data.

Statistical analysis. GraphPad Prism 5 was used for statistical data processing for the unpaired *t* test⁵⁴. Test results are indicated as the mean \pm standard error corresponding to the assay-specific three replicate mean value⁵⁵.

Conclusions

Plants and the bioactive elements found in them have drawn a lot of interest in the development and discovery of novel non-toxic, environmentally friendly methods for the synthesis of metal nanoparticles because of their superior reducing ability, anticancer properties, and physiochemical characteristics of green CuONP synthesis. The additional benefit of this technology, which outperforms conventional chemical procedures, is that it prolongs the life of NPs. The present study conducted CuONPs synthesis using green techniques. Subsequently, the nanoparticles were assessed for anticancer characteristics concerning AMJ-13, MCF-7, and HBL-100 lines to ascertain the degree of cell proliferation and apoptosis. The outcomes indicate that CuONPs demonstrated strong anti-proliferative and pro-apoptotic effects on AMJ-13 and MCF-7 cell lines. Moreover, CuONPs treatment enhanced LDH production, attributed to cell membrane destruction, causing leakage of cellular enzymes. Hence, the study suggests that the synthesised CuONPs displayed anti-proliferative behaviour that triggered cell death through apoptosis.

Data availability

The datasets used and/or analysed during the current study available from the corresponding author on reasonable request.

Received: 13 May 2022; Accepted: 12 September 2022
 Published online: 28 September 2022

References

- Barabadi, H. *et al.* Penicillium family as emerging nanofactory for biosynthesis of green nanomaterials: A journey into the world of microorganisms. *J. Clust. Sci.* **30**, 843–856 (2019).
- Saravanan, M., Barabadi, H., Ramachandran, B., Venkatraman, G. & Ponmurugan, K. Emerging plant-based anti-cancer green nanomaterials in present scenario. *Compr. Anal. Chem.* **87**, 291–318 (2019).
- AlMalki, F. A. *et al.* Eco-friendly synthesis of carbon nanoparticles by laser ablation in water and evaluation of their antibacterial activity. *J. Nanomater.* **2022**, 1–8 (2022).
- Albukhaty, S., Naderi-Manesh, H. & Tiraihi, T. In vitro labeling of neural stem cells with poly-L-lysine coated super paramagnetic nanoparticles for green fluorescent protein transfection. *Iran. Biomed. J.* **17**, 71 (2013).
- Nemati, M., Tamoradi, T. & Veisi, H. Immobilization of Gd (III) complex on Fe_3O_4 : A novel and recyclable catalyst for synthesis of tetrazole and S-S coupling. *Polyhedron* **167**, 75–84 (2019).
- Duan, H., Wang, D. & Li, Y. Green chemistry for nanoparticle synthesis. *Chem. Soc. Rev.* **44**, 5778–5792 (2015).
- Dewan, A., Sarmah, M., Thakur, A. J., Bharali, P. & Bora, U. Greener biogenic approach for the synthesis of palladium nanoparticles using papaya peel: An eco-friendly catalyst for C-C coupling reaction. *ACS Omega* **3**, 5327–5335 (2018).
- Xu, H.-J. *et al.* CuI-nanoparticles-catalyzed selective synthesis of phenols, anilines, and thiophenols from aryl halides in aqueous solution. *J. Org. Chem.* **76**, 2296–2300 (2011).
- Anandan, M. *et al.* Green synthesis of anisotropic silver nanoparticles from the aqueous leaf extract of *Dodonaea viscosa* with their antibacterial and anticancer activities. *Process Biochem.* **80**, 80–88 (2019).
- Ovais, M. *et al.* Role of plant phytochemicals and microbial enzymes in biosynthesis of metallic nanoparticles. *Appl. Microbiol. Biotechnol.* **102**, 6799–6814 (2018).
- Hosseini-Koupaei, M. *et al.* Catalytic activity, structure and stability of proteinase K in the presence of biosynthesized CuO nanoparticles. *Int. J. Biol. Macromol.* **122**, 732–744 (2019).
- Tavakoli, S., Kharaziha, M. & Ahmadi, S. Green synthesis and morphology dependent antibacterial activity of copper oxide nanoparticles. *J. Nanostruct.* **9**, 163–171 (2019).
- Berra, D. *et al.* Green synthesis of copper oxide nanoparticles by *Pheonix dactylifera* L leaves extract. *Dig. J. Nanomater. Biostruct.* **13**, 1231–1238 (2018).
- Zivadinovic, D. & Watson, C. S. Membrane estrogen receptor- α levels predict estrogen-induced ERK1/2 activation in MCF-7 cells. *Breast Cancer Res.* **7**, 1–15 (2004).
- Singh, S., Kumar, N., Kumar, M., Agarwal, A. & Mizaikoff, B. Electrochemical sensing and remediation of 4-nitrophenol using bio-synthesized copper oxide nanoparticles. *Chem. Eng. J.* **313**, 283–292 (2017).
- Sulaiman, G. M., Tawfeeq, A. T. & Jaaffer, M. D. Biogenic synthesis of copper oxide nanoparticles using *Olea europaea* leaf extract and evaluation of their toxicity activities: An in vivo and in vitro study. *Biotechnol. Prog.* **34**, 218–230 (2018).
- Nasrollahzadeh, M., Sajadi, S. M., Rostami-Vartooni, A. & Hussin, S. M. Green synthesis of CuO nanoparticles using aqueous extract of *Thymus vulgaris* L. leaves and their catalytic performance for N-arylation of indoles and amines. *J. Colloid Interface Sci.* **466**, 113–119 (2016).
- Vijay, M. & Anu, Y. Anticancer activity of camellia Sinensis mediated copper nanoparticles against HT-29, MCF-7, and MOLT-4 human cancer cell lines. *Asian J. Pharm. Clin. Res.* **10**, 71–77 (2017).
- Chung, I. M. *et al.* Green synthesis of copper nanoparticles using *Eclipta prostrata* leaves extract and their antioxidant and cytotoxic activities. *Exp. Ther. Med.* **14**, 18–24 (2017).
- Dey, A. *et al.* *Azadirachta indica* leaves mediated green synthesized copper oxide nanoparticles induce apoptosis through activation of TNF- α and caspases signaling pathway against cancer cells. *J. Saudi Chem. Soc.* **23**, 222–238 (2019).
- Rehana, D., Mahendiran, D., Kumar, R. S. & Rahiman, A. K. Evaluation of antioxidant and anticancer activity of copper oxide nanoparticles synthesized using medicinally important plant extracts. *Biomed. Pharmacother.* **89**, 1067–1077 (2017).
- Gopinath, V. *et al.* In vitro toxicity, apoptosis and antimicrobial effects of phyto-mediated copper oxide nanoparticles. *RSC Adv.* **6**, 110986–110995 (2016).
- Atawodi, S. E. in *Infectious agents and cancer*. 1–4 (Springer).
- Badrie, N. & Schauss, A. G. in *Bioactive foods in promoting health* 621–643 (Elsevier, 2010).
- Organization, W. H., Canada, P. H. A. o. & Canada, C. P. H. A. O. *Preventing chronic diseases: a vital investment*. (World Health Organization, 2005).
- George, V. C., Kumar, D., Rajkumar, V., Suresh, P. & Kumar, R. A. Quantitative assessment of the relative antineoplastic potential of the n-butanolic leaf extract of *Annona muricata* Linn. in normal and immortalized human cell lines. *Asian Pac. J. Cancer Prev.* **13**, 699–704 (2012).
- Valencia, L. *et al.* Actividad tripanocida y citotóxica de extractos de plantas colombianas. *Biomedica* **31**, 552–559 (2011).
- Nawwar, M. *et al.* Flavonol triglycoside and investigation of the antioxidant and cell stimulating activities of *Annona muricata* Linn. *Arch. Pharm. Res.* **35**, 761–767 (2012).
- Munoz-Escobar, A., Ruiz-Baltazar, Á. D. J. & Reyes-López, S. Y. Novel route of synthesis of PCL-CuONPs composites with antimicrobial properties. *Dose-Response* **17**, 1559325819869502 (2019).
- Al-Mohaiemeed, A. M., Mostafa, G. A. & El-Tohamy, M. F. New construction of functionalized CuO/ Al_2O_3 nanocomposite-based polymeric sensor for potentiometric estimation of naltrexone hydrochloride in commercial formulations. *Polymers* **13**, 4459 (2021).
- Eng, K. E., Panas, M. D., Hedestam, G. B. K. & McInerney, G. M. A novel quantitative flow cytometry-based assay for autophagy. *Autophagy* **6**, 634–641 (2010).
- Esmaeili Govarchin Ghaleh, H., Zarei, L., Mansori Motlagh, B. & Jabbari, N. Using CuO nanoparticles and hyperthermia in radiotherapy of MCF-7 cell line: Synergistic effect in cancer therapy. *Artif. Cells Nanomed. Biotechnol.* **47**, 1396–1403 (2019).
- Thamer, N. A. & Barakat, N. T. in *Journal of Physics: Conference Series*. 062104 (IOP Publishing).
- Naik, A. V. & Sellappan, K. Assessment of genotoxic potential of annonacin and *Annona muricata* L. extracts on human breast cancer (MCF-7) cells. *Adv. Tradit. Med.* **21**, 779–789 (2021).
- Naik, A. V. & Sellappan, K. In vitro evaluation of *Annona muricata* L. (Soursop) leaf methanol extracts on inhibition of tumorigenicity and metastasis of breast cancer cells. *Biomarkers* **25**, 701–710 (2020).
- Shafagh, M., Rahmani, F. & Delirezh, N. CuO nanoparticles induce cytotoxicity and apoptosis in human K562 cancer cell line via mitochondrial pathway, through reactive oxygen species and P53. *Iran. J. Basic Med. Sci.* **18**, 993 (2015).
- Khorrami, S., Zarraabi, A., Khaleghi, M., Danaei, M. & Mozafari, M. Selective cytotoxicity of green synthesized silver nanoparticles against the MCF-7 tumor cell line and their enhanced antioxidant and antimicrobial properties. *Int. J. Nanomed.* **13**, 8013 (2018).
- Vetten, M. A. *et al.* Label-free in vitro toxicity and uptake assessment of citrate stabilised gold nanoparticles in three cell lines. *Part. Fibre Toxicol.* **10**, 1–15 (2013).
- Sun, J. *et al.* Cytotoxicity, permeability, and inflammation of metal oxide nanoparticles in human cardiac microvascular endothelial cells. *Cell Biol. Toxicol.* **27**, 333–342 (2011).

40. Fu, X. Oxidative stress induced by CuO nanoparticles (CuO NPs) to human hepatocarcinoma (HepG2) cells. *J. Cancer Ther.* **6**, 889 (2015).
41. Alyamani, A. A. *et al.* Green fabrication of zinc oxide nanoparticles using phlomis leaf extract: Characterization and in vitro evaluation of cytotoxicity and antibacterial properties. *Molecules* **26**, 6140 (2021).
42. Bhuvaneshwari, V., Vaidehi, D. & Logpriya, S. Green synthesis of copper oxide nanoparticles for biological applications. *Microbiol. Curr. Res.* **2**, 9–10 (2018).
43. Hosseinzadeh, N. *et al.* Green synthesis of gold nanoparticles by using *Ferula persica* Willd. gum essential oil: Production, characterization and in vitro anti-cancer effects. *J. Pharm. Pharmacol.* **72**, 1013–1025 (2020).
44. Albukhaty, S. *et al.* Investigation of dextran-coated superparamagnetic nanoparticles for targeted vinblastine controlled release, delivery, apoptosis induction, and gene expression in pancreatic cancer cells. *Molecules* **25**, 4721 (2020).
45. Bhattacharyya, A., Chattopadhyay, R., Mitra, S. & Crowe, S. E. Oxidative stress: An essential factor in the pathogenesis of gastrointestinal mucosal diseases. *Physiol. Rev.* **94**, 329–354 (2014).
46. Chen, J. The cell-cycle arrest and apoptotic functions of p53 in tumor initiation and progression. *Cold Spring Harb. Perspect. Med.* **6**, a026104 (2016).
47. Hemalatha, G., Sivakumari, K., Rajesh, S. & Shyamala Devi, K. Phytochemical profiling, anticancer and apoptotic activity of graviola (*Annona muricata*) fruit extract against human hepatocellular carcinoma (HepG-2) cells. *Int. J. Zool. Appl. Biosci.* **5**, 32–47 (2020).
48. Al-Shammari, A. M., Al-Saadi, H., Al-Shammari, S. M. & Jabir, M. S. in *AIP Conference Proceedings*. 020206 (AIP Publishing LLC).
49. Kashan, K. S., Abdulameer, F. A., Jabir, M. S., Hadi, A. A. & Sulaiman, G. M. Anticancer activity and toxicity of carbon nanoparticles produced by pulsed laser ablation of graphite in water. *Adv. Nat. Sci. Nanosci. Nanotechnol.* **11**, 035010 (2020).
50. Al-Musawi, S. *et al.* Dextran-coated superparamagnetic nanoparticles modified with folate for targeted drug delivery of camptothecin. *Adv. Nat. Sci. Nanosci. Nanotechnol.* **11**, 045009 (2020).
51. Al-Ziyadi, A. G., Al-Shammari, A. M., Hamzah, M. I., Kadhim, H. S. & Jabir, M. S. Newcastle disease virus suppress glycolysis pathway and induce breast cancer cells death. *Viruses* **31**, 341–348 (2020).
52. Jawad, M., ÖzTÜRK, K. & Jabir, M. S. TNF- α loaded on gold nanoparticles as promising drug delivery system against proliferation of breast cancer cells. *Mater. Today Proc.* **42**, 3057–3061 (2021).
53. Jabir, M. S. *et al.* Fe_3O_4 nanoparticles capped with PEG induce apoptosis in breast cancer AMJ13 cells via mitochondrial damage and reduction of NF- κ B translocation. *J. Inorg. Organomet. Polym Mater.* **31**, 1241–1259 (2021).
54. Younus, A., Al-Ahmer, S. & Jabir, M. Evaluation of some immunological markers in children with bacterial meningitis caused by *Streptococcus pneumoniae*. *Res. J. Biotechnol.* **14**, 131–133 (2019).
55. Ali, I. H., Jabir, M. S., Al-Shmgani, H. S., Sulaiman, G. M. & Sadoon, A. H. in *Journal of Physics: Conference Series*. 012009 (IOP Publishing).

Acknowledgements

The authors extend their appreciation to the University of Technology, University of Misan, University of Baghdad, and Taif University, Researchers Supporting Project number (TURSP-2020/274) for paying the article processing charge.

Author contributions

R.I.M. and A.A.K. were concerned with conceptualization and methodology; S.I., H.S.M.-S. and R.H.A. conducted formal analysis; S.A., M.J. and M.K.A.M. were responsible for the investigation and data curation; U.N., F.A.A., G.M.S. and H.A.-K. were contributed to the study validation; R.I.M., A.A.K. and S.I. were involved in the visualization and original draft preparation; S.A., F.A.A., G.M.S. and H.A.-K. worked on writing review and editing; R.I.M. and A.A.K. and S.A. assumed supervisory responsibilities; R.I.M., A.A.K. and H.S.M.-S. were followed project administration. All authors gave approval to the final version of the manuscript.

Funding

This research received no external funding.

Competing interests

The authors declare no competing interests.

Additional information

Correspondence and requests for materials should be addressed to S.A. or M.S.J.

Reprints and permissions information is available at www.nature.com/reprints.

Publisher's note Springer Nature remains neutral with regard to jurisdictional claims in published maps and institutional affiliations.



Open Access This article is licensed under a Creative Commons Attribution 4.0 International License, which permits use, sharing, adaptation, distribution and reproduction in any medium or format, as long as you give appropriate credit to the original author(s) and the source, provide a link to the Creative Commons licence, and indicate if changes were made. The images or other third party material in this article are included in the article's Creative Commons licence, unless indicated otherwise in a credit line to the material. If material is not included in the article's Creative Commons licence and your intended use is not permitted by statutory regulation or exceeds the permitted use, you will need to obtain permission directly from the copyright holder. To view a copy of this licence, visit <http://creativecommons.org/licenses/by/4.0/>.

© The Author(s) 2022